Accumulation, Transformation, and Ionomic Responses of Platinum Nanoparticles in Rice Seedlings (*Oryza sativa L.*): Effect of Nanoparticle Diameter

Yaoyu Zhou[a], Xin Liu[a], Xiao Yang[b], Gijs Du Laing[c], Filip M. G. Tack[d], Michael S. Bank[e,f], Jochen Bundschuh[g h], Yong Sik Ok[i], Yuan Yang[a*]*

[a] College of Resources and Environment, Hunan Agricultural University, Changsha 410128, China

[b] Key Laboratory of Land Surface Pattern and Simulation, Institute of Geographic Sciences and Natural Resources Research, Chinese Academy of Sciences, Beijing 100101, China

[c] Department of Green Chemistry and Technology, Ghent University, Ghent, Belgium

[d] Department Green Chemistry and Technology, Faculty of Bioscience Engineering, Ghent University, B-9000 Gent, Belgium

[e] Institute of Marine Research, Bergen, Norway

[f] University of Massachusetts Amherst, Amherst, MA, USA

[g] Doctoral program in Science, Technology, Environment, and Mathematics. Department of Earth and Environmental Sciences, National Chung Cheng University, 168 University Rd., Min-Hsiung, Chiayi County, 62102, Taiwan, ROC

[h] School of Civil Engineering and Surveying, University of Southern Queensland, West Street, Toowoomba, 4350 Queensland, Australia

[i] Korea Biochar Research Center, O-Jeong Eco-Resilence Institute (OJERI) & Division of Environmental Science and Ecological Engineering, Korea University, Seoul 02841, Republic of Korea

*Corresponding Authors:

Yuan Yang: Email: yangyuan041@163.com; orcid.org/0000-0003-2378-8526

Yong Sik Ok: Email: yongsikok@korea.ac.kr; orcid.org/0000-0003-3401-0912

[1]

ABSTRACT: Platinum group nanoparticles (PtNPs) are increasing in the environment largely as a result of their wide use and application in automobile and medical industries. Diameter is an important property of nanoparticles and is crucial for their transport and phytotoxicity assessment. In this study, we aimed to investigate the accumulation and transformation dynamics of PtNPs with three diameters (~25 nm, ~50 nm, and ~70 nm) in rice seedlings, using multiple characterization approaches, including single-particle inductively coupled plasma mass spectrometry (SP-ICP-MS), transmission electron microscopy (TEM), and Pt total element analyses. Notably, the dissolution of small

[1] **Abbreviations:** metal nanoparticle (MNP); Single-particle inductively coupled plasma-mass spectrometry (SP-ICP-MS); platinum nanoparticle (PtNP); transmission electron microscopy (TEM); inductively coupled plasma optical emission spectrometry (ICP-OES); malondialdehyde (MDA); hierarchical cluster analysis (HCA); principal component analysis (PCA);

particles was simultaneous with the growth of the larger particles after PtNPs entered the rice tissues. Statistical and chemometric analyses, including correlation analysis, hierarchical cluster analysis, and principal component analysis, were used to identify the plant responses and element variations during PtNP treatment. The results of the combination of ionomic differentiation and PtNP uptake indicated that particle number was an important characteristic governing nanoparticle toxicity. Our study showed that combining ionomics and multiple quantitative and morphological analyses of nanoparticle accumulation are vitally important for understanding the distinctive phytotoxicity of metal nanoparticles.

KEYWORDS: Platinum nanoparticle, Rice seedling, Accumulation, Phytotoxicity, Ionomic response

1. INTRODUCTION

Metallic nanoparticles (MNPs) are widely used in agriculture, medicine, and environment remediation.[1, 2] The wide use of MNPs has inevitably resulted in their continuous release into the environment and accumulation in food webs.[3-5] The accumulation of nanoparticles (NPs) in plants, especially in crops, has recently garnered significant interest from scientists and policymakers.[6-8] The distribution and uptake of NPs depend on both plant species type and particle properties.[9, 10] In previous studies, the researchers' have focused on NP particle size.[11, 12] Notably, in plant–NP interactions, large particles are more stable than small ones.[4, 13] However, the effect of MNPs on plants is highly variable. One distinct example is MNP accumulation in wheat. Specifically, particle size-specific uptake of Ag and Au NPs significantly affects MNP

accumulation in wheat, but it does not result in enhanced phytotoxicity.[14] Other complications within this research sphere include identifying the accumulation mechanism and NP transformation and explaining their complex relationships with phytotoxicity dynamics.[15, 16]

Pt is a noble metal element, and it has a low concentration in unpolluted environment.[17, 18] However, Pt content is increasing in soils, rivers, and oceanic environments, usually as elementary nanocrystalline Pt attached to other metal particles.[19] Dispersion via road dust is the most significant source of Pt enrichment in soil ecosystems.[20, 21] PtNPs are widely used in automotive catalysts, biomedical devices, jewelry, and electrical, and glass industries.[22, 23] Previous studies have shown that Pt group nanoparticles (PtNPs) are easily transported in aquatic ecosystems and may be toxic to biota.[13, 24] However, few studies have focused on the toxicity of PtNPs in plants.[25] Sørensen et al. (2016) found that PtNPs can increase oxidative stress and growth inhibition in *P. subcapitata* than dissolved Pt.[26] NPs in soil may also interact and accumulate in plants and affecting growth.[27, 28] Recent studies have investigated the interactions between plants and NPs, such as Ag and CeO_2 NPs.[29, 30] However, the majority of these studies have focused on total metal elements rather than nanoparticle concentrations.[26, 31]

Single-particle inductively coupled plasma mass spectrometry (SP-ICP-MS) is a sophisticated method for MNP characterization and quantification.[32] Furthermore, SP-ICP-MS is a powerful tool to determine the size distribution and number of NPs at relevant environmental concentrations.[33, 34] Combined with appropriate pretreatment

methods, such as enzyme digestion, SP-ICP-MS can be used for quantitative determination of MNPs accumulated in plants, even at trace levels.[35, 36] Because of the simultaneous detection of particles and ion state signals, Sorensen et al., (2016) used SP-ICP-MS to examine the transformation between AuNPs and Au^{+} in tomato plants.

Elements are essential building blocks for cells and influence plant growth processes.[37] Environmental stresses may result in the elements variation in plants, and some elements can be transported by a protein associated with other elements and ionome responses.[38] For instance, a previous study observed Fe homeostasis in the leaf ionomes of *Arabidopsis thaliana*[39]. Significant relationships between the content of Fe in fertilizers and the content of Mn, Co, Zn, and Cd in the shoots were observed. Another study indicated that the element composition in plants varies with environmental factors[40]. Plants cope with stresses through elements network regulation[41], thus, plant ionomes—defined as mineral nutrients and trace elements in plants[39] —are sensitive to the physiological state of plants[42, 43]. Du et al. (2020) investigated the ionomic responses of rice seedlings under As stress. Their results showed that As of different valences had different influences on element accumulation in rice[44]. Ionomic responses are associated with exposed external environments [39, 45]. This study is the first to investigate the ionomic influences of MNPs in plants. Metal nanoparticles stress affects plant growth through direct accumulation, resulting in alterations in plant physiology and element variability. To effectively understand the influences of plant nutrition, it is important to investigate the total element composition in plants and the relationships between different elements, along with uptake

mechanisms and internal homeostasis in plants. However, to the best of our knowledge, few studies have investigated ionomic responses to different-sized NPs accumulated in plants.

Nevertheless, the uptake kinetics of PtNPs in rice seedlings was quantified upon exposure to different-sized PtNPs. Considering the special characteristics of MNPs, the transformation and localization of PtNPs in rice are crucial for understanding the influence of particle diameter on plant development and yield. [13, 26] Simultaneously investigating NP accumulation and ionomic responses in plants is helpful.

2. METHODS

2.1 Synthesis and Characterization of PtNPs with Three Diameters

PtNPs having three diameter sizes, PtNP-B (25 nm), PtNP-C (50 nm), and PtNP-D (70 nm), were synthesized, as described by Sikder et al [46]. Monodisperse suspensions and citrate coatings of PtNPs were prepared with regard to mixing effects and to improve stabilization for NPs, respectively. The detailed procedures used to synthetize PtNPs are provided in the Supporting Information (SI). The morphology and size distribution of the PtNPs characterized by TEM and SP-ICP-MS are shown in Figures S1 and S2. The average size comparison is shown in Table S1 and Figure S3. Notably, the average diameters of the three types of PtNPs calculated using SP-ICP-MS were 28.04 ± 3.21, 50.67 ± 2.73, and 74.11 ± 4.32 nm, respectively. Our results are in good accordance with the median diameter obtained using TEM (Figure S1), which indicated the accuracy and feasibility of the NP analyses methods used in our study. As seen in

Figure S1, PtNP-B (average diameter of 20.17 ± 4.58 nm) showed an irregularly spherical shape, while PtNP-C and PtNP-D were spherical, with diameters of 44.60 ± 3.08 and 71.59 ± 1.33 nm, respectively. The TEM results confirmed the monodispersed property of PtNPs. We used PtNP-B, PtNP-C, and PtNP-D (concentrations: 0.25, 0.5, and 1 mg/l, respectively) in plant exposure experiments. which indicated the accuracy and feasibility of the NP analysis methods used in our study. Additionally, the mass concentration of PtNPs was determined using ICP-OES and ICP-MS.

2.2 Plant Growth and Exposure Experiments

Rice seedlings (*Oryza sativa L.*) provided by the Hunan Agricultural University (Hunan province, China) were used for the experiments. To sterilize the seeds, we soaked them in 5% sodium hypochlorite solution for 15 min, flushed them with ultrapure water several times, and finally, immersed them in ultrapure water for 24 h. Sterilized seeds were germinated on moistened filter paper in a culture dish containing 20 mL ultrapure water. The culture dishes were set in an artificial climate box at 28℃ for 8 h in dark, and then, at 32℃ for 16 h in light; the relative humidity in the box was maintained at 80%.

After 5 days of cultivation, rice seedlings having a length of 2 cm were used to evaluate the influence of PtNPs on rice seedling root elongation. Suspensions of NPs having different diameters (PtNP-B: 25 nm, PtNP-C: 50 nm, and PtNP-D: 70 nm) and concentrations (0.25, 0.5, 1 mg/L, respectively) were added to 1L Hogland nutrition solution in hydroponic box. After 48 h of exposure, the average root length and weight

were measured from 10 roots of rice seedlings. The rice seedlings were harvested after 7 days of cultivation and rinsed with ultrapure water for 5 min to remove NPs adhered to the seedling roots. The samples were kept in an ultra-low temperature freezer at -80℃ until further experiments were performed.

2.3 Digestion and Content Determination of Pt and Other Elements in rice Seedlings

The rice shoots and root samples were digested in a microwave digestion system (Sineo microwave, Shanghai, China) that follows the Chinese National Standards for Food Safety Determination of multiple elements (GB5009. 268-2016). Briefly, fresh samples were added into polytetrafluoroethylene tubes and then digested using 3 mL of concentrated HNO_3 and 1 mL of HCl. The digestion protocol was as follows: first, the temperature of the system was ramped to 120°C within 5 min and this temperature was maintained for 5 min; second, the temperature was increased to150°C and maintained at this temperature for 10 min. Finally, the temperature was increased to 190°C from 150°C within 5 min and this temperature was maintained for 20 min. After digestion, all the samples were diluted to 50 mL using ultrapure water. Concentrations of 15 elements—namely, Al, B, Ca, Co, Ba, Fe, Zn, K, Mg, Mn, Pt, P, Pb, Sr, and Cu—were determined using ICP-OES (Optima 8000, Perkin Elmer, USA). Two certified reference materials—GBW10049(GSB-27) (Green Chinese onion) and GBW10020(GSB-11) (Citrus leaf)—were used to verify the accuracy of the sample pretreatment method. The detected results of certified references were in good agreement with the standard values

168 provided by manufacturer.

169

170 **2.4 Enzyme Digestion of Plant Samples**

171 Macerozyme R-10 was used to digest the plant material to release the NPs from the
172 plant matrix without destroying the NPs, according to a previous study.[35] At the same
173 time, the addition ratio of enzyme and sample was optimized to obtain a satisfying
174 extraction efficiency for the PtNPs in the rice tissues. First, 0.025 g of frozen fresh rice
175 seeding roots were ground, homogenized in 8 mL of citrate butter (2 mmol/L, pH 4.5),
176 and ultrasonicated for 5 min in an ice bath. Citric acid was applied to maintain the pH
177 at 4-5. Different amounts of macerozyme R-10 (0.0050, 0.0100, and 0.0200 g) were
178 dissolved in 2 mL ultrapure water and added to the sample solution. After 24 h of
179 homogenization in a water bath having a temperature of 37℃, the suspensions were
180 statically stratified. The supernatant liquid of these samples was diluted 1000 times
181 before determining the content of PtNPs.

182

183 **2.5 Analysis of PtNPs in Rice using SP-ICP-MS**

184 A NexION 350X (Perkin Elmer, USA) ICP-MS was used to detect the size
185 distribution, average size, and particle concentration of the PtNPs. The raw PtNPs
186 signal was processed using PerkinElmer's Syngistix software and the Nano Application
187 module. The dwell time was set at 0.1 ms and the total acquisition time was 60 s. The
188 transport efficiency of ICP-MS was measured using 50 ng/L of 60-nm Au NPs standard
189 solution (Nano Composix, Inc.). The ionic calibration of Pt was measured using a

190 standard dissolved Pt solution, with concentrations of 0.1, 0.2, 0.5, 1, and 2 μg/L. To
191 reduce particle coagulation, each sample was dispersed for 3 min using ultrasound
192 before analysis. The rice root samples were diluted 100 times after enzyme digestion,
193 and then, the particle concentration and average size were calculated, according to the
194 SP-ICP-MS analysis results. The optimized operating conditions of SP-ICP-MS are
195 shown in Table S2. The 30-nm and 60-nm PtNPs standard solutions (provided by
196 nanoComposix, Inc., USA) were used to verify the accuracy of the analysis of PtNPs
197 using SP-ICP-MS during the injection process. The particle number concentration
198 recovery of these two PtNPs standard solutions was both between 90% ± 10%, and the
199 average diameter of PtNPs detected by SP-ICP-MS was in good agree with the TEM
200 results. Both particle concentration and the average diameter of PtNPs were provided
201 by manufacturer.
202
203 **2.6 Sample detection**
204 Sample injection system should be flushed using rinse solutions (2%HNO_3 (*v/v)* and
205 ultrapure water) after the running of ICP-OES and ICP-MS. A tune solution provided
206 by PerkinElmer (USA) was used to tune the ICP-MS daily to obtain the optimal
207 condition of ICP-MS. After the calibration curve of metal element established, an
208 initial calibration verification (ICV) standard sample and calibration blank were
209 detected to verify the accuracy of initial calibration. The continuing calibration
210 verification (CCV) standard solution and continuing calibration blank (CCB) was
211 used to verify the ICP-OES and ICP-MS drift every 10 samples. For analysis of

samples, the rinse solutions (2%HNO_3 (*v/v*) and ultrapure water) were also used to flush the sample injection system before each analysis in sequence. Furthermore, the concentration of calibration blank should be less than 3 times of the method detection limit (MDL) of each element.

2.7 Statistical Analyses

Relationships between PtNPs mass concentration, particle concentration, and exposure conditions were determined using Pearson's correlation. Two-way analysis of variance (ANOVA) was conducted using SPSS Statistic 26.0 software, followed by Tukey's honest significant difference (HSD) post-hoc test. Mean concentrations were used for the analysis, and the statistical significance level was $p < 0.05$.

Multivariate statistical analyses, including correlation analysis, hierarchical cluster analysis (HCA), and principal component analysis (PCA), were carried out to reveal the ionomic response after exposure to different concentrations of PtNPs. The HCA was conducted using SPSS v.13.0 after Z-score transformation and implemented by hierarchical and Pearson distance. The PCA was performed using both Simca 14.1 and SPSS v.13.0, and a heat-map was developed using Hemi-1.0-alpha (for Windows).

3. RESULTS AND DISCUSSION

3.1 Uptake and Accumulation of Pt in Rice Tissues

The accumulation of Pt in the roots [PtNP-B (25 nm) treatment] and its transportation to the shoots [PtNP-C (50 nm) treatment] were dose-dependent and increased with

exposure concentrations (Figure S4). In the roots, the accumulation of Pt decreased when the exposure doses of PtNP-C (50 nm) and PtNP-D (70 nm) were higher than 0.5 mg/L. The relationship between the exposure conditions (i.e., particle diameter and exposure concentration) and Pt contents in the roots was evaluated using partial correlation analysis. PtNP exposure concentration and accumulated Pt content showed a significant positive correlation (r = 0.695, $p < 0.05$); no correlation was observed between the particle diameter and Pt content in the rice tissues (roots and shoots) (data available in Supplementary Information, Table S3). The diameter of PtNPs influences their uptake and transportation in rice root and shots. Both in shoot and root, Pt contents increased in a dose-dependent manner for PtNPs of small sizes [PtNP-B (25 nm) and PtNP-C (50 nm)]. However, for the large-sized particles (i.e., PtNP-D 70 nm), the Pt content was less affected by exposure concentrations (Figure S4). Previous studies also observed this difference in *Lactuca sativa*[4] and *Capsicum annuum* L.[48]. This behavior was explained by more aggregation of larger NPs compared to smaller nanoparticles, hampering their uptake in the roots and transport within the plant [4, 48].

3.2 Characterization of PtNPs in Rice Tissues using SP-ICP-MS and TEM

3.2.1 Effect of Macerozyme R-10 on PtNPs

Enzyme digestion combined with the SP-ICP-MS method provides information on size distribution and concentration of MNPs in plants[47]. This investigation is the first to apply this combined method for analysis of PtNPs in rice tissues. The enzyme digestion parameters were optimized to ensure that the extraction procedures did not

influence the morphology and diameter of the nanoparticles. The effects of macerozyme R-10 on PtNP aggregation and its dissolution in various conditions were compared (Figure S5). Figure S6 shows the measured size-distribution histogram and particle concentration of 70-nm PtNPs before and after enzyme digestion, using the optimized conditions. The results showed that particle size distribution was in good accordance with the sizes of stocked PtNPs (Figure S6). The particle concentration (7.6×10^4/mL) was close (89.3% recovery) to the particle concentration of the PtNP stock suspension (8.51×10^4/mL). These results prove that the optimized method is suitable to extract PtNPs from rice, without causing changes in diameter of the NPs.

3.2.2 Characterization of PtNPs in Rice Tissues using SP-ICP-MS

The PtNP signals in root tissues that were exposed to different treatments were determined using SP-ICP-MS (Figure 1). As seen in Figure 1(b), the signal distribution of dissolved Pt ion solution at 0.5 μg/L was small and homogeneous in SP-ICP-MS mode. Meanwhile, a large number of typical PtNP pulse signals could be found using 0.05-μg/L 50-nm PtNPs solution [Figure 1(c)][49, 50]. Compared with the raw signals of the control and ion samples, a large amount of PtNP pulse signals was observed after the sample was exposed to PtNPs [Figures 1(d–f)]. which indicated that rice roots could uptake the 25, 50, and 70-nm PtNPs. As shown in the inset figure of Figures 1(d) and 1(e), the PtNPs within the rice tissues existed as intact particles, and some of them were oxidized to Pt ions.

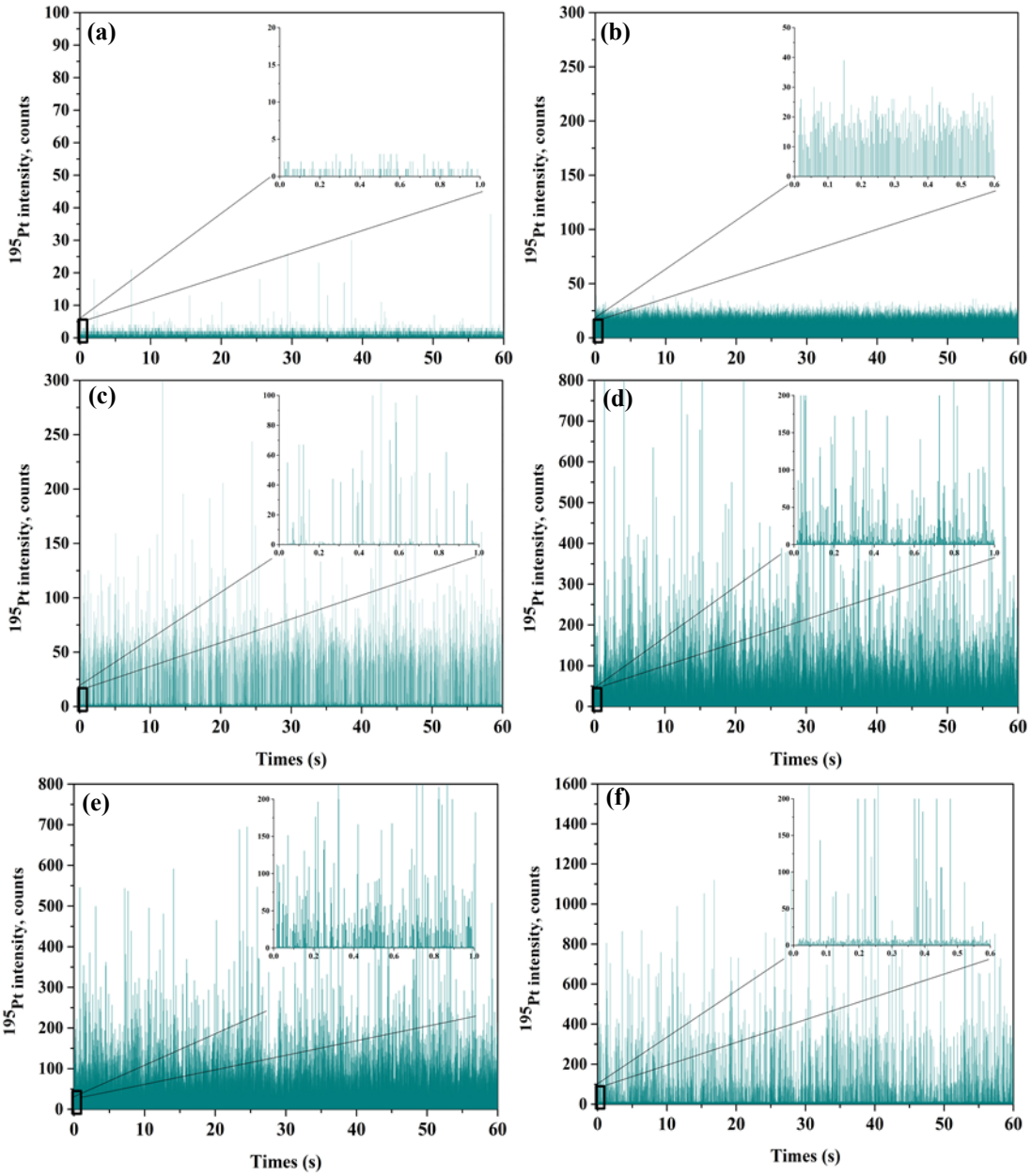

277

278 **Figure 1.** Single-particle inductively coupled plasma mass spectrometry (SP-ICP-MS)

279 raw signal of (a) control rice root, (b) 0.5 μg/L Pt ion, (c) standard 50 ng/L 50 nm PtNPs,

280 (d) 0.5 mg/L PtNP-B exposed rice-root digestates, (e) 0.5 mg/L PtNP-C exposed rice-

281 root digestates, and (f) 0.5 mg/L PtNP-D exposed rice-root digestates

282

283 The pulse signals in SP-ICP-MS can be due to absorption or uptake of PtNPs into

284 the rice root, and the continuous signal can be due to the dissolution of these PtNPs in

root tissue. In addition, there were almost no dissolved Pt signals in the sample of rice root with PtNP-D exposure (Figure 1f), and the pulse signals excluded the particle dissolution of PtNP-D. These results indicate that the dissolution of PtNPs is more likely for small-sized NPs than for large-sized NPs. Hence, particle size was a significant driver of the transformation of the NPs. These results are in good agreement with those of previous studies[51, 52] that reported that the ion release from MNPs is size-dependent (Zhang et al., 2010). For example, Schwabe et al. (2014) found that, under the same conditions, small-sized (9 nm) CeO_2 NPs were not stable and dissolved more readily than large-sized NPs (64 nm) in root[51].

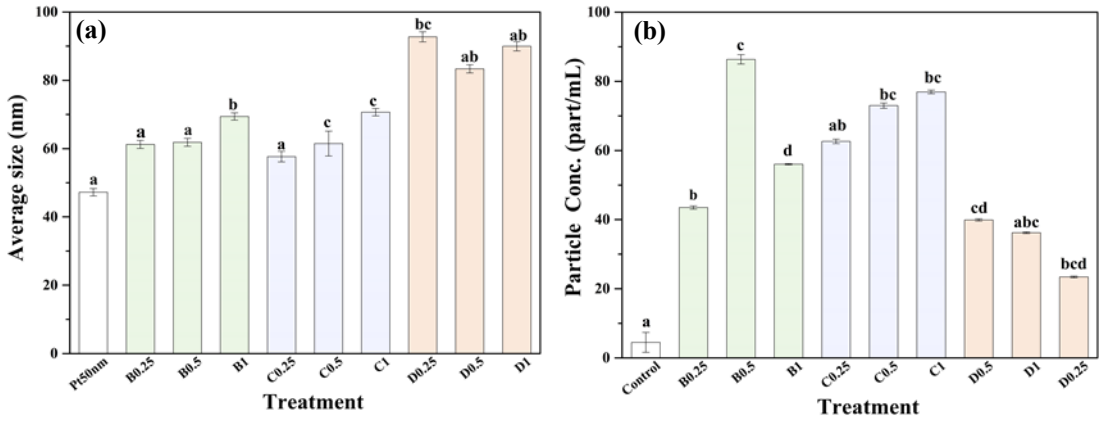

Figure 2. (a) Average particle size and (b) Particle concentration of PtNPs in rice roots exposed to different PtNP treatments ($n = 3$). Different upper-case and lower-case letters represent statistical differences at $p < 0.01$ for different foliar and root exposure treatments, respectively. The treatment B0.25 stands for the exposure to PtNP-B with 0.25mg/L

The calculated particle concentrations and average particle diameters of PtNPs in rice roots obtained from PtNPs treated with different concentration levels (0.25, 0.5,

303 and 1 mg L^{-1}) and diameters [PtNP-B (25 nm), PtNP-C (50 nm), PtNP-D (70 nm)] are
304 shown in Figure 2. Compared with the initial particle diameter [PtNP-B (25 nm), PtNP-
305 C (50 nm), PtNP-D (70 nm)], the particle diameter in the plant increased to ~60, ~70,
306 and ~90 nm (for PtNP-B, PtNP-C, and PtNP-D, respectively), indicating that the
307 particles in the rice roots were aggregated during all of the treatments. In addition,
308 exposure concentration of PtNPs seemed to have fewer effects on the particle size of
309 the NPs in rice roots. Besides, the aggregations of small-sized PtNPs are more
310 significant than large-sized PtNPs. Results of particle concentrations showed that the
311 amount of PtNP was higher during the PtNP-C (50 nm) treatment than those during the
312 PtNP-B (25 nm) and PtNP-D (70 nm) treatments. For large-sized PtNP treatment, the
313 particle number concentrations decreased with increasing exposure concentrations,
314 which could be attributed to particle aggregation. These results contradict those
315 observed in studies of other MNPs[4, 35]. This is because, in general, the previous studies
316 focused on the total content, instead of the NP concentration[54], and the total content
317 included dissolved and particle states. Conversely, our results indicate that the total
318 content accumulation of Pt in rice roots is dependent on exposure mass concentrations
319 of PtNPs. The highest total Pt content in the rice roots upon exposure to PtNP-B
320 corresponded to a low particle concentration, which was also evidence of PtNP-B
321 dissolution.

322 *3.2.3 Cell Damage and PtNP Transformation during Interaction with the Cell Wall*

323 To understand the PtNP uptake at a cellular level, NPs taken up by the root tips
324 exposed to PtNP-D (~75 nm) were characterized using TEM. As shown in Figure 3,

PtNPs were absorbed by the cell and distributed around the cell wall. The effects of PtNPs on plant cell structure led to cell membrane rupture and contraction. As shown in Figure 5c, some of the intracellular NPs agglomerated significantly when the diameters of the nanoparticles were ~400 nm and the extracellular NPs maintained the original size (below 100 nm). These results indicate that NPs exhibit different transformations inside and outside the rice root cells. The root surface is a critical interface for physicochemical interactions between NPs and plants, mainly for a variety of root exudates including organic acid, phenolics, and other small molecular substances[55]. We postulate that PtNPs absorbed into the root surface, especially in the case of the roots exposed to small-sized PtNPs, could be dissolved and these interactions are more likely to occur inside than outside the root cells. The large-sized PtNPs inside the plant cell could be explained by recrystallization. The dissolved Pt ions were deposited on the surface of particles and dissolution of small particles with the simultaneous growth of the larger particles.

This observation was in contrast with the findings of a previous study regarding CeO_2 transformation in hydroponic cucumber, which showed that the transformation of NPs occurred only outside the plant tissues[56]. The root exudates (such as organic acid and phenolics) were considered important factors in the metal–NP transformation process[57, 58]. The intracellular aggregation of the PtNPs could be attributed to the polysaccharide macromolecules and metal ions in the cytoplasm, which is consistent with AgNP aggeregation promoted by exopolysaccharide macromolecules and divalent cations[59].

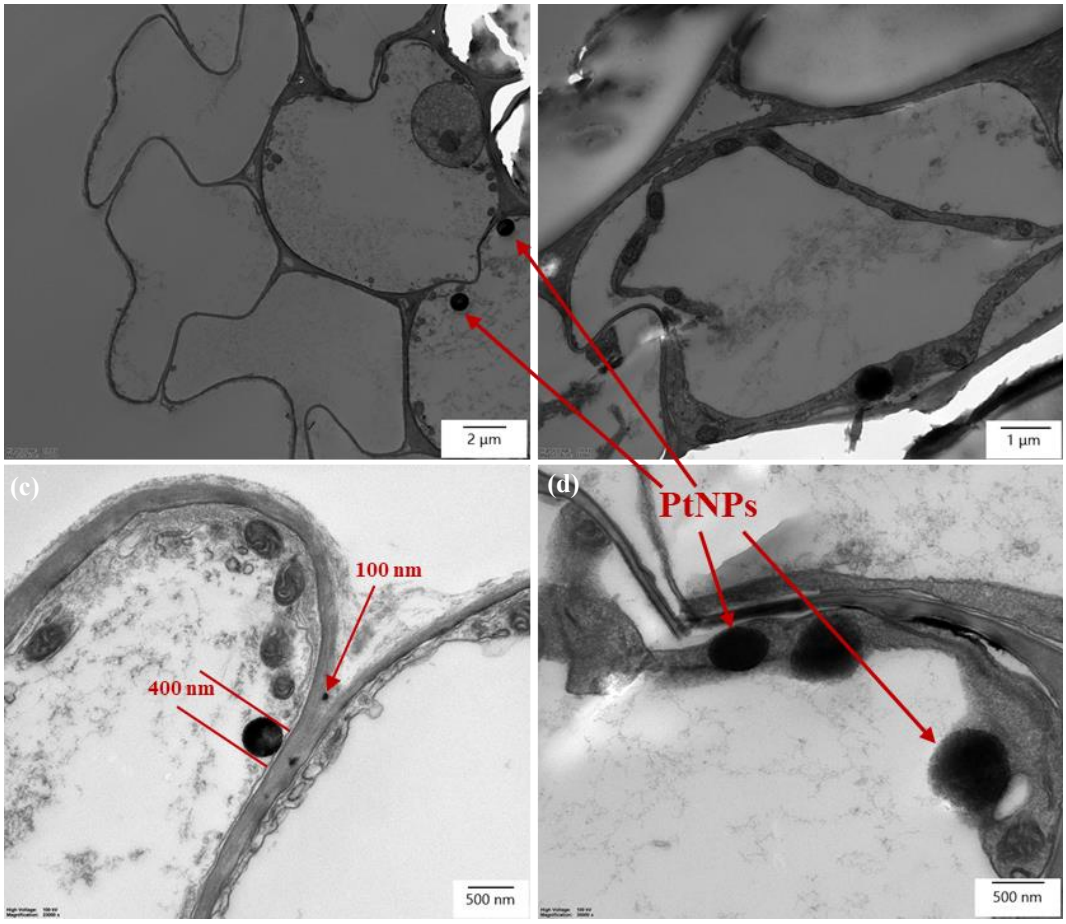

Figure 3. Transmission electron microscopy (TEM) images of root tip after 3-day exposure to PtNP-C (size 70 nm; concentration 1 mg/L); Platinum group nanoparticles (PtNPs)

3.3 Influences on Root Elongation and Biomass

To test the toxicity of particle size and concentration of PtNPs, the elongation and biomass of rice seedlings were compared after 3 days of exposure to PtNP-50 (Figure S7). Exposed to PtNPs of different diameters exhibited similar effects on plant growth. Following an increase in the exposure dose, the fresh plant-biomass of the roots and shoots declined without concentration dependence. This observation differed from that of other studies on NP phytotoxicity; the other studies showed a trend of decreasing

biomass with a decrease in exposure dose. Notably, the exposure concentration level is critical for influencing plant growth. Specifically, biomass production increased when exposing the rice to increasing PtNPs levels below 0.5 mg/L; but when the exposure exceeded 0.5 mg/L, inhibition effects occurred, with increasing exposure dosages decreasing the biomass production of the shoots and roots. Compared with the control sample, the shoot length decreased by 11, 17, and 21% during PtNP-C exposure and 47, 31, and 44% during PtNP-D exposure of 1, 2, and 5-mg/L PtNP treatment over control, respectively. These results indicate that PtNPs can inhibit the growth of the rice seedlings, especially with respect to biomass accumulation and root elongation, which might affect the yield of rice. Different influences were observed for different particle diameters. An inhibiting effect on plant growth was also observed when the plant was exposed to other MNPs. For example, exposure to AgNPs significantly decreased the biomass of soybean and rice seedlings[60].

To further explore the oxidative toxicity of PtNPs on the growth of rice seedlings and the different responses to NPs, we tested the activity of antioxidant enzyme peroxidase and malondialdehyde (MDA) content in rice seedlings under the exposure of PtNP of various sizes. Notably, high MDA content reflects the damage to cell membrane. As shown in Figure S8, exposure to lower concentrations of PtNP-D (70 nm) resulted in higher MDA contents compared to exposure to higher concentrations of the same particles. Moreover, exposure to intermediate sized particles (PtNP-C, 50 nm) showed stronger oxidant damage and toxicity than exposure to other sizes of particles. This can possibly be attributed to the fact that the particle number concentration of PtNP-C (50

nm) accumulated in the roots of the seedlings which was the highest among the three particle types (Figure S8). These results indicate that increased phytotoxicity is likely caused by the increasing number of PtNPs in the rice roots. We thus hypothesize that the influences of the size of the PtNPs on phytotoxicity could be explained by the differences in particle numbers accumulated within the rice cells.

3.4 Ionomic Variations Assessed by Multivariate Statistical Analyses

3.4.1 Element Contents in Rice Tissues

Previous studies have shown that element content is related to plant tissue types [61-63]. Additionally, ionomic profiles are sensitive to environmental stresses [44, 64]. In this study, the contents of 15 elements in the roots and shoots of the rice seedlings were studied after the plant was exposed to NPs with different diameters and concentrations (Figure S9). In the root tissue, mineral nutrients significantly decreased with PtNP exposure, which varied according to the concentration and particle size of NPs, and the relationships between the different elements require further investigation to elucidate the responsible mechanisms. In the shoots, the contents of Pb, Ba, Al, B, and Fe varied when there was a high degree of larger particle-size PtNP concentrations, compared with that observed in control samples. To better understand the variations in different elements after exposure to PtNPs, the data were then subjected to further statistical and chemometric analyses.

3.4.2 Correlation Analyses

Correlation analyses were applied to investigate the relationships between the 15 essential elements (in the roots and shoots) (Figure 4). In the shoots and roots, we observed a weak correlation between Pt and other elements. The data are listed in Table S4. The correlations between the elements were stronger in the shoots than the roots. Hence, shoot ionomes may be considered better indicators of plant growth and stress responses. As seen in Figures 4(a) and 4(b), in the rice roots, Pt content showed a distinct correlation to Cu content (r = -0.7791, $p < 0.01$), and in the shoot tissue, we observed a negative correlation to the Fe content (r = -0.5515, $p < 0.05$). The negative correlations between Pt and other elements (except for Co) indicate that PtNP stress inhibited element accumulation in rice seedlings.

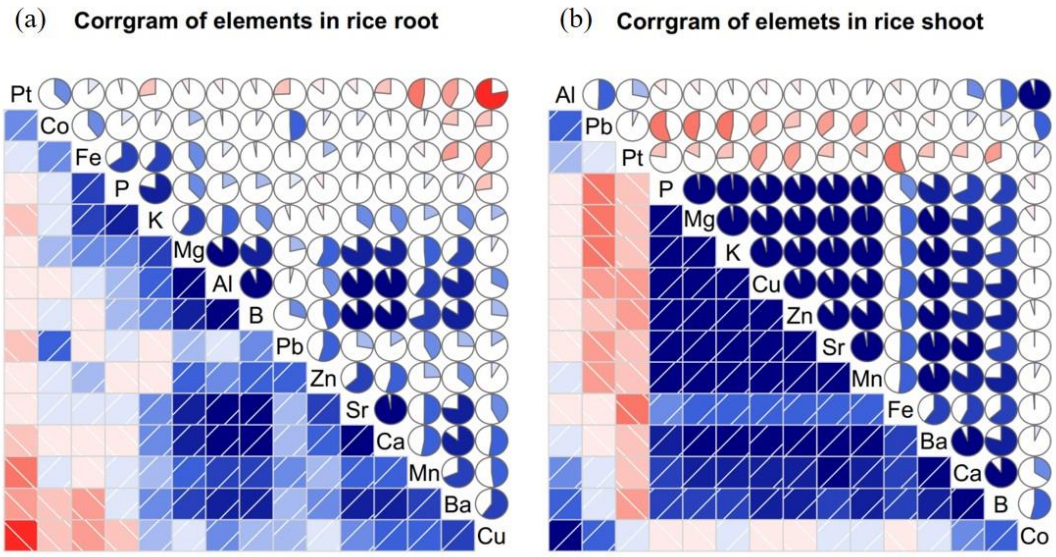

Figure 4. Correlation analysis of elements in PtNP-exposed rice tissue: (a) Root and (b) Shoot. The colors red and blue represent negative and positive correlation, respectively. The area of sector in each little pie chart indicates the correlation coefficient (r); the larger color sector indicates a stronger correlation between the two elements.

We identified several important correlations among mineral nutrients and particular trace elements in rice shoots. The essential macronutrients (K, Ca, Mg, P) and micronutrients (Cu, Zn, Mn, B) were positively correlated with each other (Table S4). Among these mineral nutrients, Fe, correlated with Zn, K, and Mg in rice and maize shoots, and is considered essential for plant growth and development[65, 66]. These correlation results indicate that PtNP exposure significantly influences Fe concentration in the rice shoots. Previous studies also established that in *Arabidopsis,* Fe response was associated with environment perturbations[39]. Notably, PtNP-exposure breaks down Fe homeostasis, but the mechanism of PtNP influence on Fe transport in plants requires further investigation. In summary, we found that Fe homeostasis was strongly affected by PtNP treatment.

3.4.3 HCA and PCA for Ionomic Responses of Rice Seedlings

HCA and PCA were performed to further understand the ionomic responses to PtNPs. As shown in Figure 5, two-way dendrograms generated from HCA are illustrated as heatmaps. The heatmaps show contents after uniformization for improved comparisons of different elements and the maps red color indicates samples with higher Pt content and green denotes those with lower Pt content. In vertical HCA between various treatments, the samples were categorized into two distinctive groups, namely, the root and the shoot clusters. Under PtNP stress, the elements accumulated more in the roots than in the shoots, except for some macro-elements such as K, P, Mn, and Mg. In the root cluster, samples were further classified into two groups. One group had PtNPs of large diameters at high concentrations and the other group had PtNPs of small diameters

438 with low concentrations, like the control group without PtNP exposure. These results
439 further indicate that exposure doses and particle diameters significantly affect the
440 accumulation of PtNPs in the roots. However, there were no significant differences
441 between the two groups. Specifically, macro-elements (e.g., K, P, Mn, and Mg)
442 exhibited little distinction between the two groups. Some elements such as Al, B, Sr,
443 Ca, and Ba expressed diameter dependence; these elements were released less for the
444 PtNP-D (70 nm)-exposed group than for the other groups. In the shoot cluster, PtNP-D
445 (70 nm; 1 mg/L) samples were separated from others. These samples were classified
446 into two distinct clusters: samples with an exposure dose of 0.5 mg/L PtNPs and those
447 with other exposure doses. The content of elements in the shoots changed slightly after
448 PtNP exposure. In the horizontal HCA between various elements, the elements were
449 classified into four groups: 1) Zn; 2) K, Mn, P, and Mg; 3) Pt, Fe, and Co; and 4) other
450 elements. Fe was considered a relevant element for Pt accumulation content, which is
451 consistent with the correlation analyses results.

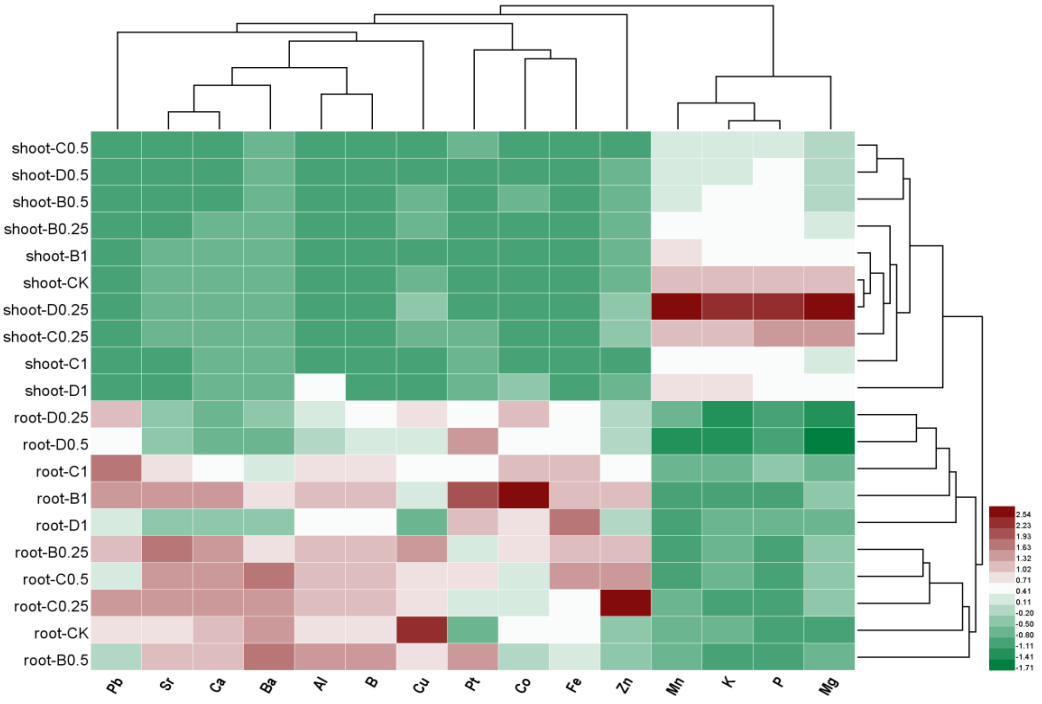

Figure 5. Hierarchical cluster analysis (HCA) analyses for element content in PtNP-treated rice tissues. The treatment like root-B0.25 stands for the root samples exposure to PtNP-B with 0.25mg/L.

The PCA study was performed for further exploratory analysis. PCA could reduce the dimensionality of datasets[67]; the first two PCs were enough to explain 86.8 % of the total variance (Figure 6a). A major difference was observed between the ionomes of the roots and shoots. The loading plots of the 15 elements (Figure 6b) indicated that the elements were split into three groups; there was a strong negative correlation between Pt and K, P, Mg, and Mn, which agreed with previous results obtained from correlation analyses and HCA. To identify the dominant factors responsible for the ionome covariance corresponding to PtNP stress, the classifications of the NP content and

diameter are compared in Figures 6(c) and 6(d). The first two PCs explained 81.1% of the total variance and were highly responsive to treatment conditions. From the comparison of classifications in Figures 6(c) and 6(d), when plotting the score with PC1 and PC2, the lines from each treatment cluster together with a more distinct separation between exposure concentration than PtNPs diameter. The results showed that shoot ionomes were primarily affected by PtNP concentrations; the diameter of the exposed PtNPs also affected the rice plant ionomes. The score plots of root ionomes are shown in Figure S10, which indicated that the larger size PtNP treatments [PtNP-D (70 nm)] were different from other PtNPs treatment in rice roots. However, there was no significant difference between the PtNP-B (25 nm) and PtNP-C (50 nm) treatments.

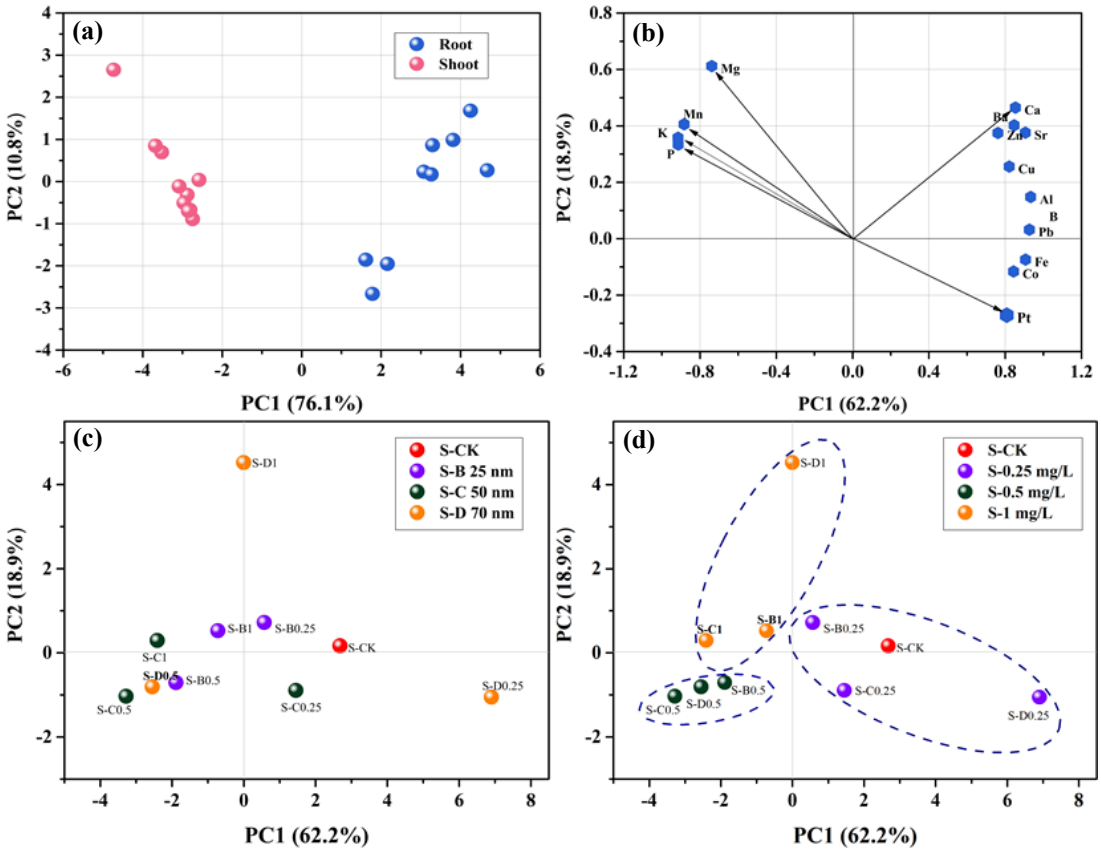

Figure 6. Score plot of principal component analysis (PCA) for: (a) all samples, b) loading plot for all samples, (c) shoot samples with particle size, and (d) concentration

Combined with the previous deduction about PtNP accumulation in rice root, we can firmly attest to the fact the diameter of the PtNPs influenced the particle transformation. Notably, the phytotoxicity of PtNPs was closely associated with their accumulation in rice roots. We found that the difference in rice plant development and the ionomic responses between the various exposure conditions can be attributed to the characteristics of PtNPs.

4. CONCLUSIONS AND FUTURE WORK

In this study, we demonstrated that the uptake, transformation, and phytotoxicity of PtNPs in rice are influenced by their size and exposure concentration. The small-sized PtNPs (25 nm and 50 nm) accumulated in rice after entering the plant tissues and absorbed on the root surface. We could deduce that the NPs entered the plant cells and their aggregation damaged the cell structure since part of the particles were further translocated to the shoots (around 10% of root accumulated). The particles absorbed on the root surface were highly likely to partially break down into smaller particles and dissolve as Pt ions. Particles have grown due to deposition of Pt ions on existing particles, dissolution of small particles with the simultaneous growth of the larger particles after PtNPs entered the rice tissues. Multiple analyses demonstrated that PtNP treatment caused variation of elements essential for the rice seedlings as a response to environmental changes. A significant concentration-dependence was observed for upward translocation of Pt when the plant was exposed to PtNPs, resulting in PtNP-induced rice growth reduction and phytotoxicity. The phytotoxicity effects, including

cell structure damage, oxidative damage, and elongation inhibition, were closely related to particle number concentration—instead of the total Pt content—in rice roots. Therefore, the influences of PtNP size on phytotoxicity could be attributed to different particle number concentration of the treatments. Studying ionomes with respect to metabolic and genomic responses might be important to understand plant detoxification mechanisms after PtNP exposure. We believe this to be an ideal direction for future studies. Notably, our results provide a valuable reference dataset for further investigations on the effect of MNPs of different diameters on plant ionomes.

Author Contributions

Yaoyu Zhou: Resources, methodology, writing (review and editing), and visualization; Xin Liu: Data collection, methodology, writing, and visualization; Xiao Yang: Writing (review and editing); Gijs Du Laing: Writing (review and editing), Filip M. G. Tack: Writing (review and editing), Jochen Bundschuh: Writing (review and editing), Michael S. Bank: Writing (review and editing); Yong Sik Ok: Conceptualization, writing (review and editing), and supervision; Yuan Yang: Conceptualization, writing (review and editing), and supervision.

Conflicts of interest

The authors declare no competing financial interests.

Acknowledgments

The study was financially supported by the National Natural Science Foundation of China (Grant No. 42107308 and 51709103); the China Postdoctoral Science Foundation (Grant No. 2019M652768), the National Natural Science Foundation of Hunan province (Grant No. 2020JJ5227 and 2020JJ5259); the Hunan Provincial Key R&D (Grant No. 2019WK2031); and the Research Foundation of Education Bureau of Hunan Province (Grant No.20A239).

REFERENCES

1. Deng, Y.; Petersen, E. J.; Challis, K. E.; Rabb, S. A.; Holbrook, R. D.; Ranville, J. F.; Nelson, B. C.; Xing, B., Multiple method analysis of tio_2 nanoparticle uptake in rice (*Oryza sativa L.*) plants. *Environ. Sci. Technol.* **2017,** *51*, (18), 10615-10623.

2. Liang, C.; Xiao, H.; Hu, Z.; Zhang, X.; Hu, J., Uptake, transportation, and accumulation of C_{60} fullerene and heavy metal ions (Cd, Cu, and Pb) in rice plants grown in an agricultural soil. *Environ. Pollut.* **2018,** *235*, 330-338.

3. Wu, Y.; Yang, L.; Gong, H.; Dang, F.; Zhou, D. M., Contrasting effects of iron plaque on the bioavailability of metallic and sulfidized silver nanoparticles to rice. *Environ. Pollut.* **2020,** *260*, 113969.

4. Torrent, L.; Iglesias, M.; Margui, E.; Hidalgo, M.; Verdaguer, D.; Llorens, L.; Kodre, A.; Kavcic, A.; Vogel-Mikus, K., Uptake, translocation and ligand of silver in Lactuca sativa exposed to silver nanoparticles of different size, coatings and concentration. *J. Hazard. Mater.* **2020,** *384,* 121201.

5. Zhai, G.; Gutowski, S. M.; Walters, K. S.; Yan, B.; Schnoor, J. L., Charge, size, and cellular selectivity for multiwall carbon nanotubes by maize and soybean. *Environ. Sci. Technol.* **2015,** *49*, 7380-7390.

6. Trujillo-Reyes, J.; Majumdar, S.; Botez, C. E.; Peralta-Videa, J. R.; Gardea-Torresdey, J. L., Exposure studies of core-shell Fe/Fe(3)O(4) and Cu/CuO NPs to lettuce (*Lactuca sativa*) plants: Are they a potential physiological and nutritional hazard? *J. Hazard. Mater.* **2014,** *267*, 255-263.

7. Hussain, A.; Ali, S.; Rizwan, M.; Zia Ur Rehman, M.; Javed, M. R.; Imran, M.; Chatha, S. A. S.; Nazir, R., Zinc oxide nanoparticles alter the wheat physiological response and reduce the cadmium uptake by plants. *Environ. Pollut.* **2018,** *242*, 1518-1526.

8. Xiao, W.; Hao, Z.; Jian, Z.; Xianxiang, L.; Zhenyu, W.; Baoshan, X., Photodegradation elevated the toxicity of polystyrene microplastics to grouper (*Epinephelus moara*) through disrupting hepatic lipid homeostasis. *Environ. Sci. Technol.* **2020**, *54*, 6202-6212.

9. Zhang, P.; Guo, Z.; Luo, W.; Monikh, F. A.; Xie, C.; Valsami-Jones, E.; Lynch, I.; Zhang, Z., Graphene oxide-induced pH alteration, iron overload, and subsequent oxidative damage in rice (*Oryza sativa* L.): a new mechanism of nanomaterial phytotoxicity. *Environ. Sci. Technol.* **2020**, *54*, 3181-3190.

10. Zhu, Z. J.; Wang, H. H.; Yan, B.; Zheng, H.; Jiang, Y.; Miranda, O. R.; Rotello,

V. M.; Xing, B. S.; Vachet, R. W., Effect of surface charge on the uptake and distribution of gold nanoparticles in four plant species. *Environ. Sci. Technol.* **2012,** *46*, (22), 12391-12398.

11. Yanyu, B.; Chengrong, P.; Weitao, L.; Yunxia, L.; Chuanxin, M.; Baoshan, X., Iron plaque reduces cerium uptake and translocation in rice seedlings (*Oryza sativa* L.) exposed to CeO_2 nanoparticles with different sizes. *Sci. Total Environ.* **2019**, 661, 767-777.

12. Falco, W. F.; Scherer, M. D.; Oliveira, S. L.; Wender, H.; Colbeck, I.; Lawson, T.; Caires, A. R. L., Phytotoxicity of silver nanoparticles on Vicia faba: Evaluation of particle size effects on photosynthetic performance and leaf gas exchange. *Sci. Total Environ.* **2020,** *701*, 134816.

13. Sikder, M.; Croteau, M.-N.; Poulin, B. A.; Baalousha, M., Effect of nanoparticle size and natural organic matter composition on the bioavailability of polyvinylpyrrolidone-coated platinum nanoparticles to a model freshwater invertebrate. *Environ. Sci. Technol.* **2021,** *55*, (4), 2452-2461.

14. Zhang, W. Y.; Wang, Q.; Li, M.; Dang, F.; Zhou, D. M., Nonselective uptake of silver and gold nanoparticles by wheat. *Nanotoxicology* **2019,** *13*, (8), 1073-1086.

15. Le, Y.; Feiran, C.; Kaiqiang, Y.; Zhenggao, X.; Xiaoyu, Y.; Zhenyu, W.; Baoshan, X., Early development of apoplastic barriers and molecular mechanisms in juvenile maize roots in response to La_2O_3 nanoparticles. *Sci. Total Environ.* **2019**, *653*,

675-683.

16. Zhenyu, W.; Lei, Z.; Jian, Z.; Baoshan, X., Environmental processes and toxicity of metallic nanoparticles in aquatic systems as affected by natural organic matter†. *Environ. Sci.: Nano* **2016**, *3*, 240-255.

17. Barbosa, J. R.; Paranhos, C. H.; Alves, O. C.; Checca, N. R.; Serna, J. P.; Rossi, A. L.; Silva, J. C. M., Low loading platinum dispersed on Ni/C nanoparticles as high active catalysts for urea electrooxidation reaction. *Electrochim. Acta* **2020,** *355*, 136752.

18. Zhu, J.; Hu, S.; Zeng, Z.; Li, W.-X., First-principles investigation of electrochemical dissolution of Pt nanoparticles and kinetic simulation. *J. Chem. Phys.* **2019,** *151*, 234711.

19. Książyk, M.; Asztemborska, M.; Stęborowski, R.; Bystrzejewska-Piotrowska, G., Toxic effect of silver and platinum nanoparticles toward the freshwater microalga pseudokirchneriella subcapitata. *Bull. Environ. Contam. Toxicol.* **2015,** *94*, 554-558.

20. Merget, R.; Rosner, G., Evaluation of the health risk of platinum group metals emitted from automotive catalytic converters. *Sci. Total Environ.* **2001,** *270*, (1), 165-173.

21. Reith, F.; Campbell, S. G.; Ball, A. S.; Pring, A.; Southam, G., Platinum in earth surface environments. *Earth Sci. Rev.* **2014,** *131*, 1-21.

22. Pei, W.; Liu, Y.; Deng, J.; Zhang, K.; Hou, Z.; Zhao, X.; Dai, H., Partially embedding Pt nanoparticles in the skeleton of 3DOM Mn_2O_3: An effective strategy for

601 enhancing catalytic stability in toluene combustion. *Appl. Catal. B: Environ.* **2019,** *256*,
602 117814.

603 23. Carnis, J.; Gao, L.; Fernández, S.; Chahine, G.; Schülli, T. U.; Labat, S.;
604 Hensen, E. J. M.; Thomas, O.; Hofmann, J. P.; Richard, M.-I., Facet-dependent strain
605 determination in electrochemically synthetized platinum model catalytic nanoparticles.
606 *Small* **2021**, *17*, 2007702.

607 24. Demir, V.; Bucher, J.; Kropf, C.; Arenz, M.; Segner, H., Comparative study of
608 cytotoxicity by platinum nanoparticles and ions in vitro systems based on fish cell lines.
609 *Toxicol. In Vitro* **2020,** *66*, 104859.

610 25. Kranjc, E.; Mazej, D.; Regvar, M.; Drobne, D.; Remskar, M., Foliar surface
611 free energy affects platinum nanoparticle adhesion, uptake, and translocation from
612 leaves to roots in arugula and escarole. *Environ. Sci. Nano* **2018,** *5*, 520-532.

613 26. Sorensen, S. N.; Engelbrekt, C.; Lutzhoft, H. H.; Jimenez-Lamana, J.; Noori,
614 J. S.; Alatraktchi, F. A.; Delgado, C. G.; Slaveykova, V. I.; Baun, A., A multimethod
615 approach for investigating algal toxicity of platinum nanoparticles. *Environ. Sci.*
616 *Technol.* **2016,** *50*, (19), 10635-10643.

617 27. Yasur, J.; Rani, P. U., Environmental effects of nanosilver: impact on castor
618 seed germination, seedling growth, and plant physiology. *Environ. Sci. Pollut. Res.*
619 **2013,** *20*, 8636-8648.

620 28. Lv, J. T.; Zhang, S. Z.; Luo, L.; Zhang, J.; Yang, K.; Christie, P., Accumulation,

621 speciation and uptake pathway of ZnO nanoparticles in maize. *Environ. Sci. Nano* **2015,**
622 *2*, 68-77.

623 29. Chen, Z. W.; Sheng, X. L.; Wang, J.; Wen, Y. Z., Silver nanoparticles or free
624 silver ions work? An enantioselective phytotoxicity study with a chiral tool. *Sci. Total*
625 *Environ.* **2018,** *610*, 77-83.

626 30. Chuanxin, M.; Sudesh, C.; Baoshan, X.; Craig, M.; Jason, C. W.; Om Parkash,
627 D., Physiological and molecular response of *Arabidopsis thaliana (L.)* to nanoparticle
628 cerium and indium oxide exposure. *ACS Sustainable Chem. Eng.* **2013**, *7*, 768-778.

629 31. Gawronska, H.; Przybysz, A.; Szalacha, E.; Pawlak, K.; Brama, K.; Miszczak,
630 A.; Stankiewicz-Kosyl, M.; Gawronski, S. W., Platinum uptake, distribution and
631 toxicity in Arabidopsis thaliana L. plants. *Ecotoxicol. Environ. Saf.* **2018**, *147*, 982-989.

632 32. Prichard, H. M.; Fisher, P. C., Identification of platinum and palladium
633 particles emitted from vehicles and dispersed into the surface environment. *Environ.*
634 *Sci. Technol.* **2012,** *46*, 3149-3154.

635 33. Dan, Y. B.; Zhang, W. L.; Xue, R. M.; Ma, X. M.; Stephan, C.; Shi, H. L.,
636 Characterization of gold nanoparticle uptake by tomato plants using enzymatic
637 extraction followed by single-particle inductively coupled plasma-mass spectrometry
638 analysis. *Environ. Sci. Technol.* **2015,** *49*, 3007-3014.

639 34. Lee, S.; Bi, X.; Reed, R. B.; Ranville, J. F.; Herckes, P.; Westerhoff, P.,
640 Nanoparticle size detection limits by single particle ICP-MS for 40 elements. *Environ.*

641 *Sci. Technol.* **2014,** *48*, 10291-10300.

642 35. Wei, W.-J.; Li, L.; Gao, Y.-P.; Wang, Q.; Zhou, Y.-Y.; Liu, X.; Yang, Y., Enzyme
643 digestion combined with SP-ICP-MS analysis to characterize the bioaccumulation of
644 gold nanoparticles by mustard and lettuce plants. *Sci. Total Environ.* **2021,** *777*, 146038.

645 36. Li, L.; Wang, Q.; Yang, Y.; Luo, L.; Ding, R.; Yang, Z.-G.; Li, H.-P., Extraction
646 method development for quantitative detection of silver nanoparticles in environmental
647 soils and sediments by single particle inductively coupled plasma mass spectrometry.
648 *Anal. Chem.* **2019,** *91*, 9442-9450.

649 37. Baxter, I., Ionomics: The functional genomics of elements. *Brief. Funct.*
650 *Genomics* **2010,** *9*, (2), 149-156.

651 38. Baxter, I.; Dilkes, B. P., Elemental profiles reflect plant adaptations to the
652 environment. *Science* **2012,** *336*, 1661-1663.

653 39. Baxter, I. R.; Vitek, O.; Lahner, B.; Muthukumar, B.; Borghi, M.; Morrissey,
654 J.; Guerinot, M. L.; Salt, D. E., The leaf ionome as a multivariable system to detect a
655 plant's physiological status. *Proc. Natl. Acad. Sci.U.S.A* **2008,** *105*, 12081.

656 40. Campos, A. C. A. L.; Kruijer, W.; Alexander, R.; Akkers, R. C.; Danku, J.; Salt,
657 D. E.; Aarts, M. G. M., Natural variation in *Arabidopsis thaliana* reveals shoot ionome,
658 biomass, and gene expression changes as biomarkers for zinc deficiency tolerance. *J.*
659 *Exp. Bot.* **2017,** *68*, 3643-3656.

660 41. Ramírez-Flores, M. R.; Rellán-Álvarez, R.; Wozniak, B.; Gebreselassie, M.-

661 N.; Jakobsen, I.; Olalde-Portugal, V.; Baxter, I.; Paszkowski, U.; Sawers, R. J. H., Co-
662 ordinated changes in the accumulation of metal ions in maize (*Zea mays ssp. mays L.*)
663 in response to inoculation with the arbuscular mycorrhizal fungus funneliformis
664 mosseae. *Plant Cell Physiol.* **2017,** *58*, 1689-1699.

665 42. Yuan, J.; Sun, N.; Du, H.; Muhammad, U.; Kang, H.; Du, B.; Yin, S.; Liu, C.,
666 Correlated metabolic and elemental variations between the leaves and seeds of oak trees
667 at contrasting geologically derived phosphorus sites. *Sci. Total Environ.* **2019,** *691*, 178-
668 186.

669 43. Martínez-Oró, D.; Párraga-Aguado, I.; Querejeta, J.-I.; Álvarez-Rogel, J.;
670 Conesa, H. M., Nutrient limitation determines the suitability of a municipal organic
671 waste for phytomanaging metal(loid) enriched mine tailings with a pine-grass co-
672 culture. *Chemosphere* **2019,** *214*, 436-444.

673 44. Du, F.; Liu, P.; Wang, K.; Yang, Z.; Wang, L., Ionomic responses of rice plants
674 to the stresses of different arsenic species in hydroponics. *Chemosphere* **2020,** *243*,
675 125398.

676 45. Zhang, C.; Hiradate, S.; Kusumoto, Y.; Morita, S.; Koyanagi, T. F.; Chu, Q.;
677 Watanabe, T., Ionomic responses of local plant species to natural edaphic mineral
678 variations. *Front. Plant Sci.*, **2021,** *12*, 614613.

679 46. Sikder, M.; Wang, J.; Chandler, G. T.; Berti, D.; Baalousha, M., Synthesis,
680 characterization, and environmental behaviors of monodispersed platinum

681 nanoparticles. *J. Colloid Interface Sci.* **2019,** *540*, 330-341.

682 47. Wei, W. J.; Li, L.; Gao, Y. P.; Wang, Q.; Zhou, Y. Y.; Liu, X.; Yang, Y., Enzyme
683 digestion combined with SP-ICP-MS analysis to characterize the bioaccumulation of
684 gold nanoparticles by mustard and lettuce plants. *Sci. Total Environ.* **2021,** *777*, 146038.

685 48. Vinković, T.; Novák, O.; Strnad, M.; Goessler, W.; Jurašin, D. D.; Parađiković,
686 N.; Vrček, I. V., Cytokinin response in pepper plants (*Capsicum annuum L.*) exposed to
687 silver nanoparticles. *Environ. Res.* **2017,** *156*, 10-18.

688 49. Yang, Y.; Long, C.-L.; Li, H.-P.; Wang, Q.; Yang, Z.-G., Analysis of silver and
689 gold nanoparticles in environmental water using single particle-inductively coupled
690 plasma-mass spectrometry. *Sci. Total Environ.* **2016,** *563-564*, 996-1007.

691 50. Yang, Y.; Long, C.-L.; Yang, Z.-G.; Li, H.-P.; Wang, Q., Characterization and
692 determination of silver nanoparticle using single particle-inductively coupled plasma-
693 mass spectrometry. *Chin. J. Anal. Chem.* **2014,** *42*, 1553-1560.

694 51. Schwabe, F.; Schulin, R.; Rupper, P.; Rotzetter, A.; Stark, W.; Nowack, B.,
695 Dissolution and transformation of cerium oxide nanoparticles in plant growth media. *J*
696 *Nanopart. Res.* **2014,** *16*, 2668 .

697 52. Sandbeck, D. J. S.; Inaba, M.; Quinson, J.; Bucher, J.; Zana, A.; Arenz, M.;
698 Cherevko, S., Particle size effect on platinum dissolution: practical considerations for
699 fuel cells. *ACS Appl. Mater. Interfaces* **2020,** *12*, (23), 25718-25727.

700 53. Zhang, H.; Chen, B.; Banfield, J. F., Particle size and pH effects on

701 nanoparticle dissolution. *J. Phys. Chem. C* **2010,** *114*, 14876-14884.

702 54. Avellan, A.; Yun, J.; Zhang, Y.; Spielman-Sun, E.; Unrine, J. M.; Thieme, J.;
703 Li, J.; Lombi, E.; Bland, G.; Lowry, G. V., Nanoparticle size and coating chemistry
704 control foliar uptake pathways, translocation, and leaf-to-rhizosphere transport in wheat.
705 *ACS Nano* **2019,** *13*, 5291-5305.

706 55. Liu, M.; Feng, S.; Ma, Y.; Xie, C.; He, X.; Ding, Y.; Zhang, J.; Luo, W.; Zheng,
707 L.; Chen, D.; Yang, F.; Chai, Z.; Zhao, Y.; Zhang, Z., Influence of surface charge on the
708 phytotoxicity, transformation, and translocation of CeO_2 nanoparticles in cucumber
709 plants. *ACS Appl. Mater. Interfaces* **2019,** *11*, 16905-16913.

710 56. Ma, Y.; Zhang, P.; Zhang, Z.; He, X.; Zhang, J.; Ding, Y.; Zhang, J.; Zheng, L.;
711 Guo, Z.; Zhang, L.; Chai, Z.; Zhao, Y., Where does the transformation of precipitated
712 ceria nanoparticles in hydroponic plants take place? *Environ. Sci. Technol.* **2015,** *49*,
713 10667-10674.

714 57. Zhang, P.; Ma, Y.; Xie, C.; Guo, Z.; He, X.; Valsami-Jones, E.; Lynch, I.; Luo,
715 W.; Zheng, L.; Zhang, Z., Plant species-dependent transformation and translocation of
716 ceria nanoparticles. *Environ. Sci. Nano* **2019,** *6*, 60-67.

717 58. Barton, L. E.; Auffan, M.; Bertrand, M.; Barakat, M.; Santaella, C.; Masion,
718 A.; Borschneck, D.; Olivi, L.; Roche, N.; Wiesner, M. R.; Bottero, J.-Y., Transformation
719 of pristine and citrate-functionalized CeO_2 nanoparticles in a laboratory-scale activated
720 sludge reactor. *Environ. Sci. Technol.* **2014,** *48*, 7289-7296.

721 59. Chen, W.; Song, J.; Jiang, S.; He, Q.; Ma, J.; Huangfu, X. Influence of
722 extracellular polymeric substances from activated sludge on the aggregation kinetics of
723 silver and silver sulfide nanoparticles. *Front. Environ. Sci. Eng.* **2021**, 16, 16.

724 60. Li, C. C.; Dang, F.; Li, M.; Zhu, M.; Zhong, H.; Hintelmann, H.; Zhou, D. M.,
725 Effects of exposure pathways on the accumulation and phytotoxicity of silver
726 nanoparticles in soybean and rice. *Nanotoxicology* **2017,** *11*, 699-709.

727 61. Brizio, P.; Benedetto, A.; Squadrone, S.; Curcio, A.; Pellegrino, M.; Ferrero,
728 M.; Abete, M. C., Heavy metals and essential elements in Italian cereals. *Food Addit.*
729 *Contam. Part B* **2016,** *9*, (4), 261-267.

730 62. Jeyasingh, P. D.; Goos, J. M.; Thompson, S. K.; Godwin, C. M.; Cotner, J. B.,
731 Ecological Stoichiometry beyond Redfield: An Ionomic Perspective on Elemental
732 Homeostasis. *Front. Microbiol.* **2017,** *8*, 722-729.

733 63. Marquès, M.; Sierra, J.; Drotikova, T.; Mari, M.; Nadal, M.; Domingo, J. L.,
734 Concentrations of polycyclic aromatic hydrocarbons and trace elements in Arctic soils:
735 A case-study in Svalbard. *Environ. Res.* **2017,** *159*, 202-211.

736 64. Yang, M.; Lu, K.; Zhao, F.-J.; Xie, W.; Ramakrishna, P.; Wang, G.; Du, Q.;
737 Liang, L.; Sun, C.; Zhao, H.; Zhang, Z.; Liu, Z.; Tian, J.; Huang, X.-Y.; Wang, W.; Dong,
738 H.; Hu, J.; Ming, L.; Xing, Y.; Wang, G.; Xiao, J.; Salt, D. E.; Lian, X., Genome-wide
739 association studies reveal the genetic basis of ionomic variation in rice. *Plant Cell* **2018**,
740 *30*, 2720-2740.

741 65. Stich, B.; Benke, A.; Schmidt, M.; Urbany, C.; Shi, R.; von Wirén, N., The
742 maize shoot ionome: Its interaction partners, predictive power, and genetic
743 determinants. *Plant Cell Environ.* **2020**, *43*, (9), 2095-2111.

744 66. Xiao, W.; Liu, P.; Wang, K.; Yang, Z.; Wang, L., Relationship between
745 ionomics and transcriptomics of rice plant in response to arsenite stress. *Environ. Exp.*
746 *Bot.* **2021**, *189*, 104565.

747 67. De La Cruz, A. R. H.; De La Cruz, J. K. H.; Tolentino, D. A.; Gioda, A., Trace
748 element biomonitoring in the Peruvian andes metropolitan region using Flavoparmelia
749 caperata lichen. *Chemosphere* **2018,** *210*, 849-858.

750